Original Article

Assessment of coronary computed tomography angiography-derived plaque features in the diagnosis of optical coherence tomography-defined vulnerable plaques

Xiaojing Liu[1,2]^, Ruigang Xie[1], Yukun Pan[1], Zhihan Xu[3], Yinghui Ge[1], Junling Xu[2]

[1]Department of Radiology, Zhengzhou University People's Hospital, Fuwai Central China Cardiovascular Hospital, Zhengzhou, China; [2]Department of Nuclear Medicine, Henan Key Laboratory of Novel Molecular Probes and Clinical Translation in Nuclear Medicine, Henan Provincial People's Hospital & Zhengzhou University People's Hospital, Zhengzhou, China; [3]Siemens Healthineers CT Collaboration, Shanghai, China

Contributions: (I) Conception and design: X Liu, R Xie, J Xu; (II) Administrative support: X Liu, Y Ge; (III) Provision of study materials or patients: R Xie, Y Pan, J Xu; (IV) Collection and assembly of data: X Liu, Y Pan, Z Xu; (V) Data analysis and interpretation: X Liu, Y Pan, Z Xu, Y Ge; (VI) Manuscript writing: All authors; (VII) Final approval of manuscript: All authors.

Correspondence to: Yinghui Ge, MD, PhD. Department of Radiology, Zhengzhou University People's Hospital, Fuwai Central China Cardiovascular Hospital, No. 1 Fuwai Road, Zhengzhou 451460, China. Email: cjr.geyinghui@zzu.edu.cn; Junling Xu, MD, PhD. Department of Nuclear Medicine, Henan Key Laboratory of Novel Molecular Probes and Clinical Translation in Nuclear Medicine, Henan Provincial People's Hospital & Zhengzhou University People's Hospital, No. 7 Weiwu Road, Zhengzhou 450003, China. Email: xjlhzq@163.com.

Background: Identification of vulnerable plaque is essential for pre-estimation of the risk of cardiovascular disease (CVD) and stratification of major adverse cardiac events (MACEs) risks. This study aimed to evaluate the diagnostic ability of coronary computed tomography angiography (CCTA)-derived qualitative and quantitative plaque features in detecting optical coherence tomography (OCT)-defined vulnerable plaques.

Methods: A total of 31 patients who underwent both CCTA and OCT were retrospectively included in this study. The results of OCT and CCTA were blindly analyzed on a segment-to-segment comparison. The qualitative and quantitative plaque parameters derived by CCTA were recorded. Univariate analysis and multivariate logistic regression analysis were performed to reveal the independent predictors. The diagnostic efficacy of quantitative parameters was evaluated by receiver operating characteristic (ROC) curve and area under the curve (AUC).

Results: A total of 76 plaques in 31 patients were included for analysis, of which 15/76 plaques (19.7%, 10 patients) were vulnerable plaques. Low-density plaques, spotty calcification (SC), positive remodeling (PR), number of high-risk plaque signs, non-calcified fraction, and lipid fraction displayed significant differences between vulnerable and non-vulnerable plaques ($P<0.05$). Fibrotic plaque volume (FPV) [odds ratio (OR) =1.013; 95% confidence interval (CI): 1.003–1.024] and low attenuation plaque (LAP) (OR =23.416; 95% CI: 4.725–116.055) were shown to be independent predictors of vulnerable plaques. Compared with qualitative and quantitative models, the mixed model integrating all significant CCTA-derived plaque characteristics achieved the highest AUC and accuracy (mixed model AUC =0.87, 95% CI: 0.808–0.979; qualitative model AUC =0.80, 95% CI: 0.654–0.941; quantitative model AUC =0.64, 95% CI: 0.528–0.866).

Conclusions: The CCTA-derived plaque characteristics were able to detect the OCT-defined vulnerable plaques and show great potential as a non-invasive biomarker for early diagnosis of coronary vulnerable plaques.

Keywords: Major adverse cardiac events (MACEs); coronary computed tomography angiography (CCTA); optical

^ ORCID: 0000-0003-4604-8117.

coherence tomography (OCT); vulnerable plaques; plaque features

Submitted Apr 25, 2024. Accepted for publication Jan 10, 2025. Published online Feb 17, 2025.
doi: 10.21037/qims-24-838
View this article at: https://dx.doi.org/10.21037/qims-24-838

Introduction

Cardiovascular disease (CVD) is the leading cause of death worldwide, with high morbidity and mortality. According to the World Health Organization (WHO), approximately 177 million people die each year from CVD, with heart attacks and strokes accounting for 80% of these deaths (1). In China, the prevalence of CVD has increased in recent years. Plaque formation on the coronary vessel wall, followed by rupture, causes coronary artery occlusive disease and acute cardiovascular events, such as acute heart attack, which are life-threatening (2). Identification of vulnerable plaques is critical for predicting the risk of CVD and stratifying the risks of major adverse cardiac events (MACEs).

Optical coherence tomography (OCT) can clearly display the coronary plaque microstructure with a spatial resolution of 10–20 μm through near-infrared light and reconstruct recognizable intravascular images with accurate quantified plaque composition (3). The characteristics of atherosclerotic plaques identified using OCT have been reported to be consistent with histopathological results, a phenomenon known as "optical biopsy" (4). However, due to the high cost and complexity of OCT, it is not widely used.

Recently, coronary computed tomography angiography (CCTA) has become the gold standard for screening medium- and low-risk coronary heart diseases (5). CCTA is a unique non-invasive anatomical tool that allows for robust assessment of CVD including qualitative, semi-quantitative, or quantitative parameters, and has emerged as an excellent gatekeeper for invasive coronary angiography. CCTA can detect the characteristics of ruptured plaques and judge high-risk signs, such as positive remodeling (PR), low attenuation plaque (LAP), spotty calcification (SC), and napkin-ring sign (NRS) (6). Furthermore, it offers unique advantages in the quantitative analysis of plaque composition and volume (7). Nonetheless, using OCT as a control, only a few studies on quantitative coronary plaque analysis have used OCT as a control, most of which have focused on identifying thin-cap fibroatheroma (TCFA) defined by OCT (7-9). The present study aimed to evaluate the ability of CCTA-derived qualitative and quantitative plaque features to detect OCT-defined vulnerable plaques. We present this article in accordance with the STROBE reporting checklist (available at https://qims.amegroups.com/article/view/10.21037/qims-24-838/rc).

Methods

Study population

The study was conducted in accordance with the Declaration of Helsinki (as revised in 2013). The study was approved by the Ethics Board of Fuwai Central China Cardiovascular Hospital (2019 Ethical Review No. 9) and the requirement for individual consent for this retrospective analysis was waived. Patients who had undergone both CCTA and OCT at Fuwai Central China Cardiovascular Hospital from December 2018 to February 2022 were retrospectively analyzed in this study. The exclusion criteria of patients were as follows: (I) extensive calcified plaques in coronary vessels with a lumen stenosis degree of ≥95%; (II) fragmentary or low image quality CCTA and OCT examination data; (III) percutaneous coronary intervention performed prior to CCTA and OCT examinations; and (IV) an interval of more than 4 weeks between CCTA and OCT examinations.

Image acquisition

OCT was used to analyze the causes of lesions in order to improve interventional treatment strategies. To prevent catheter-induced coronary spasm, heparinized anticoagulation and intracoronary nitroglycerin (100–200 μg) were routinely administered prior to OCT imaging. After initializing the OCT imaging system (Light Lab C7 XR^{TM}; LightLab Imaging, Westford, MA, USA), creating a new case, preparing the C7 Dragonfly imaging catheter (St. Jude Medical, St. Paul, MN, USA), and connecting this catheter to the drive motor and optical controller and an integrated drive motor and optical controller, image acquisition begins after acquiring test images and verifying calibration.

A conventional angioplasty guidewire (0.014 inches) was advanced to the distal end of the lesion and then a C7 Dragonfly imaging catheter was inserted at least 10 mm from the lesion. Images were acquired using an automatic retraction device at 20 mm/s.

A dual-source CT scanner (SOMATOM Force CT; Siemens Healthineers, Erlangen, Germany) was used for image acquisition. None of the patients took drugs to reduce heart rate or dilate blood vessels, and their heart rate was controlled within 90 beats per minute under natural conditions. First, a calcium scoring scan was performed to determine the calcification burden of each blood vessel. Prospective electrocardiogated serial scanning was used in all patients, the time window of 30–80% R-R interval was collected, the automatic tube voltage (CARE kV; Siemens Healthineers), automatic tube current (CARE Dose 4D; Siemens Healthineers), and the speed was 0.25 s/rot. Using a dual-barrel power injector, a bolus of contrast media (55–60 mL) was injected into the antecubital vein at a rate of 4–5 mL/s, followed by a 30–40 mL saline flush. Intelligent tracking technology was adopted to track the descending aorta root and trigger automatically when the threshold value of 100 Hounsfield units (HU) was reached. A scanning delay of 6 s was implemented. The reconstruction layer was 0.75 mm thick and the reconstruction interval was 0.5 mm. The CT system automatically reconstructed optimal diastolic and systolic data at 0.75 mm thickness and Bv44 convolution kernel. After scanning and reconstruction, the data was transferred to the workstation for multi-plane reconstruction (MPR), including coronal and sagittal images, combined with maximum intensity projection (MIP) and volume reconstruction (VR).

Image analysis

OCT analysis was performed using the OCT imaging system (Light Lab C7 XR^{TM}) by experienced observers who were blinded to the outcomes of the CCTA. OCT image observation indicators include TCFA, plaque rupture, thrombus, and calcified nodules. Based on the results of the OCT image analysis, all plaques were classified as high-risk plaques or non-high-risk plaques. Plaques showing the signs of TCFA, plaque rupture, calcified nodules, and thrombus were defined as high-risk plaques, whereas plaques that did not show these signs were defined as non-high-risk plaques (10,11). Lipid-rich plaques with thin fibrous caps (minimum thickness <65 μm) were defined as TCFA; discontinuity of thin fibrous caps with localized cavitation was defined as plaque rupture; irregular masses that adhered to the luminal surface or floated within the lumen were defined as thrombi; and nodular calcifications protruding into the lumen with rupture of the fibrous cap and sometimes thrombosis were defined as calcified nodules (12).

Qualitative analysis of CCTA images was performed using a workstation (Syngo.Via, VB20; Siemens Healthineers). The qualitative indicators of CCTA plaques included PR, LAP, SC, NRS, and number of vulnerable plaques signs. PR was defined as the ratio of the largest vessel diameter in the segment where the plaque was located to the proximal reference vessel diameter of ≥1.12. LAP was defined as the presence of any component with a CT value <30 HU within the plaque. SC was defined as the presence of calcified plaque with a diameter <3 mm in any direction, length of the calcium less than 1.5 times the vessel diameter, and width of the calcification <2/3 of the vessel diameter (13). NRS is characterized by a low-density plaque core surrounded by high-density annular shadows (14). The number of vulnerable plaques signs was defined as the number of signs of vulnerable plaques present at the same time on a plaque.

Quantitative analysis of CCTA images was performed using a software (Coronary Plaque Analysis 4.2.0; Siemens Healthineers). To ensure consistency of plaque location assessment using CCTA and OCT, the distances between the segment where the plaque is located and the opening of the coronary vessel and the surrounding branches were set as anatomical landmarks for judgment. Both ends of the plaque were manually determined; manual adjustments were implemented if the identification of the lumen and wall was not accurate. According to the CT threshold (HU), plaque components were classified as follows: lipid plaques, −100 to 30 HU; fibrous plaques, 30 to 190 HU; and calcified plaques, >190 HU (15). Plaque quantitative indicators include plaque burden (PB), calcified plaque volume (CPV), calcified plaque ratio (CP%), non-CPV (NCPV), non-calcified plaque ratio (NCP%), fibrotic plaque volume (FPV), fibrotic plaque ratio (FP%), lipid plaque volume (LPV), lipid plaque ratio (LP%), minimum lumen area (MLA), eccentricity index (EI), stenosis rate (SR), and remodeling index (RI). The plaque components ratio was defined as the percentage of plaque volume of each component in total plaque volume (plaque volume of each component/total plaque volume × 100%). PB was defined as the ratio of plaque volume to blood vessel volume.

The results of the OCT and CCTA were compared blindly on a segment-to-segment basis. The same two

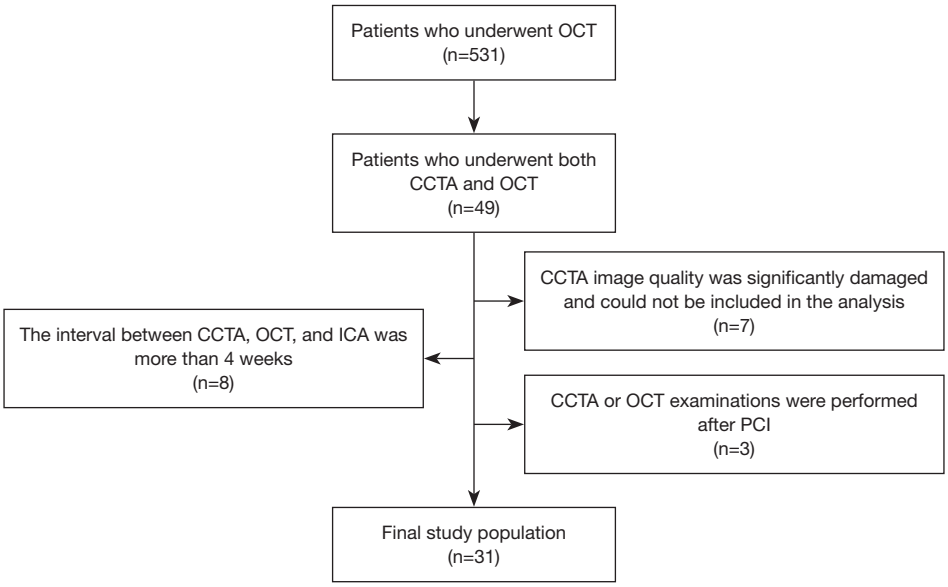

Figure 1 Flowchart of patient inclusion. A total of 49 patients who had undergone both CCTA and OCT were reviewed. Finally, 31 patients, including 24 males and 7 females, with CVD were included. OCT, optical coherence tomography; CCTA, coronary computed tomography angiography; ICA, invasive coronary angiography; PCI, percutaneous coronary intervention; CVD, cardiovascular disease.

senior radiologists reviewed the data retrospectively, and qualitative and quantitative plaque parameters derived from CCTA were recorded. Finally, the evaluation results were checked for consistency. The quantitative parameters were evaluated using intraclass correlation coefficient (ICC), whereas the qualitative parameters were evaluated using Coehn's kappa.

Statistical analysis

The software SPSS 23.0 (IBM Corp., Armonk, NY, USA) and R (version 3.6.1; R Foundation for Statistical Computing, Boston, MA, USA) were used for statistical analysis. Continuous variables were expressed as mean with standard deviation (conforming to normal distribution) or median with interquartile range (non-normal distribution), and categorical variables were expressed as percentage (%). Kappa agreement and ICC were used to assess interobserver agreement. For between-group comparisons of quantitative variables, independent *t*-test and Mann-Whitney *U* test were used, whereas for between-group comparisons of categorical variables, Chi-squared test and Fisher's exact test were used. To identify independent factors for detecting OCT-defined vulnerable plaques, univariate and multivariate logistic regression analyses were performed with a stepwise approach. A P value of <0.1 in univariate analysis was used as the inclusion criterion for the multivariate logistic analysis. The diagnostic efficacy of parameters was evaluated using the receiver operating characteristic (ROC) curve, area under the curve (AUC), accuracy, sensitivity, and specificity. The optimal cutoff was determined using the Youden's index, and differences between AUCs were determined using Delong's test. A P value of <0.05 was considered statistically significant.

Results

Patient characteristics

At the beginning, 49 patients who had undergone both CCTA and OCT were reviewed. Among these patients, 8 who had experienced a time interval of more than 4 weeks between CCTA, OCT, and ICA examination; 7 who had CCTA image quality that was significantly damaged; and 3 for whom CCTA or OCT was performed after coronary intervention were excluded from this study. Finally, 31 patients, including 24 males and 7 females, with CVD were included (*Figure 1*). The age of the analyzed patients ranged from 39 to 77 years, with a mean age of 57.7±10.6 years. A total of 76 plaques were analyzed, with 15 vulnerable plaques meeting the OCT definition and 61 nonvulnerable plaques meeting the OCT definition. There

Table 1 CVD patients' baseline characteristics

Variables	Non-vulnerable plaques (n=21)	Vulnerable plaques (n=10)	P value
Age (years)	57.9±9.8	56.3±11.4	0.468
Sex (male)	18 [86]	7 [70]	0.358
Hypertension	14 [67]	6 [60]	0.717
Hypercholesterolemia	6 [29]	4 [40]	0.685
Diabetes	4 [19]	3 [30]	0.652
Smokers	6 [29]	4 [40]	0.685
BMI ≥28 kg/m^2	3 [14]	4 [40]	0.172

Values are mean ± standard deviation or n [%]. CVD, cardiovascular disease; BMI, body mass index.

were no significant differences in the distribution of clinical characteristics, such as age, gender, obesity, and chronic disease history, between vulnerable and nonvulnerable plaque cases (P>0.05) (*Table 1*). The number of vulnerable plaques distributed in the left anterior descending (LAD), left circumflex (LCX), and right coronary artery (RCA) was 7, 2, and 6, whereas the number of non-vulnerable plaques was 47, 8, and 6, respectively. Plaques localization in the LAD and RCA differed between vulnerable and nonvulnerable plaque groups.

Analysis of differences in CCTA parameters between vulnerable and nonvulnerable plaques

The quantitative parameters evaluated using ICC were >0.85, whereas the qualitative parameters calculated using kappa were >0.75.

When LAP, SC, PR, number of high-risk plaque signs, NCP%, and LP% were compared between the vulnerable and nonvulnerable plaque groups, a statistically significant difference was observed (P<0.05). However, no significant differences in the NRS, PB, CPV, NCPV, FPV, FP%, LPV, MLA, EI, SR, and RI were observed between the two groups (*Table 2*, *Figures 2*,*3*).

Independent predictors

Univariate analysis showed that SC, LAP, PR, NCPV, NCP%, LP%, and FPV were potential predictors of vulnerable plaques (P<0.1) (*Table 3* and *Figure 4*).

The qualitative model was constructed by incorporating parameters with P<0.1 from the single factor analysis, and the qualitative indicators were derived using stepwise regression. Ultimately, SC [odds ratio (OR) =4.521; 95% confidence interval (CI): 1.022–20.008] and LAP (OR =8.012; 95% CI: 2.024–31.718) remained as significant parameters in the qualitative model. The quantitative model was constructed using a multi-factor backward stepwise approach, with LP% (OR =1.148; 95% CI: 0.993–1.327) being the sole remaining quantitative variable. A mixed model combining both qualitative and quantitative indicators was constructed using stepwise regression analysis, resulting in FPV (OR =1.013; 95% CI: 1.003–1.024) and LAP (OR =23.416; 95% CI: 4.725–116.055) remaining (*Table 4*).

Efficacy evaluation of models based on different parameters of CCTA in diagnosing vulnerable plaques

Compared with qualitative and quantitative models, a mixed model (LAP and FPV) established based on screening of all CCTA parameters had the highest AUC [mixed model, AUC =0.87, 95% CI: 0.808–0.979; qualitative model (PC and LAP), AUC =0.80, 95% CI: 0.654–0.941; and quantitative model (LP%), AUC =0.64, 95% CI: 0.528–0.866]. ROC curve evaluation of the three models revealed that the AUC of the mixed model was significantly higher than that of the qualitative model (DeLong's test: P=0.022), and the diagnostic performance evaluation of the quantitative and qualitative models compared with the mixed model showed statistical significance (McNemar test, P<0.05) (*Table 5* and *Figure 5*).

Discussion

In the present study, due to the limited availability of diagnostic and treatment procedures, there was a scarcity of cases presenting both OCT plaques and preoperative

Table 2 Comparison of vulnerable and non-vulnerable plaques with qualitative and quantitative parameters

Variables	Vulnerable plaques (n=15)	Non-vulnerable plaques (n=61)	P value
NRS	6 [40]	17 [28]	0.365
SC	7 [47]	6 [10]	0.003
LAP	9 [60]	7 [11]	<0.001
PR	9 [60]	19 [31]	0.039
Number of vulnerable plaques signs	2±2	0±2	<0.001
PB	0.62±0.25	0.64±0.16	0.243
CPV (m^3)	35.6±41.47	37.17±56.6	0.725
CP%	35.98±18.83	38.42±23.59	0.563
NCPV (m^3)	93.49±135.59	58.8±71.17	0.208
NCP%	64.02±18.83	63.1±21.82	0.044
LPV (m^3)	0.52±9.21	0.13±1.77	0.178
LP%	0.8±9.2	0.1±2	0.046
FPV (m^3)	92.97±136.14	58.74±68.14	0.264
FP%	63.05±18.46	60.26±20.72	0.061
MLA (m^2)	3.52±5.39	2.97±3.3	0.7
RI	0.98±0.63	1.06±0.69	0.306
EI	0.37±0.28	0.34±0.36	0.638
SR (%)	32.51±59.14	26.72±39.05	0.238

The data for (NRS, SC, LAP, and PR) are presented as number [%], whereas the number of vulnerable plaque signs is presented as the median with interquartile range, other variables not specified are presented as mean ± standard deviation. For between-group comparisons of categorical variables (NRS, SC, LAP, PR, and number of vulnerable plaques signs), Chi-squared test and Fisher's exact test were used, whereas for between-group comparisons of quantitative variables (PB, CPV, CP%, and others were not noted), independent *t*-test and Mann-Whitney *U* test were used. Number of vulnerable plaques signs is vulnerable plaque number that a plaque had at the same time. NRS, napkin-ring sign; SC, spotty calcification; LAP, low attenuation plaque; PR, positive remodeling; PB, plaque burden; CPV, calcified plaque volume; CP%, calcified plaque ratio; NCPV, non-calcified plaque volume; NCP%, non-calcified plaque ratio; LPV, lipid plaque volume; LP%, lipid plaque ratio; FPV, fibrotic plaque volume; FP%, fibrotic plaque ratio; MLA, minimum lumen area; RI, remodeling index; EI, eccentricity index; SR, stenosis rate.

CCTA, resulting in a small sample size. Ultimately, analysis of 76 plaques in 31 patients using CCTA and OCT revealed that (I) when OCT results were used as a reference, FPV and LAP were independent indicators of high-risk and non-high-risk plaques. (II) Compared with using qualitative or quantitative parameters alone to diagnose vulnerable plaques, a mixed model based on all qualitative and quantitative meaningful parameters showed better diagnostic performance.

OCT has long been considered the gold standard for plaque quantification and characterization. However, it is invasive and its application is limited to specific lesions. CCTA is a more appealing alternative to intravascular imaging because it allows noninvasive plaque assessment in the whole coronary tree in a diverse population. A recent serial study demonstrated that the qualitative and quantitative plaque features derived from CCTA were consistent with those derived from OCT (16). The combination of lesion location and the presence of high-risk plaque characteristics, including PR, LAP, SC, and the NRS, enables CCTA to provide valuable indications regarding lesion risk (17).

In this study, we found that LAP, SC, and PR were significantly different between the vulnerable and nonvulnerable plaque groups. Moreover, SC could serve as a potential independent predictor for diagnosing vulnerable

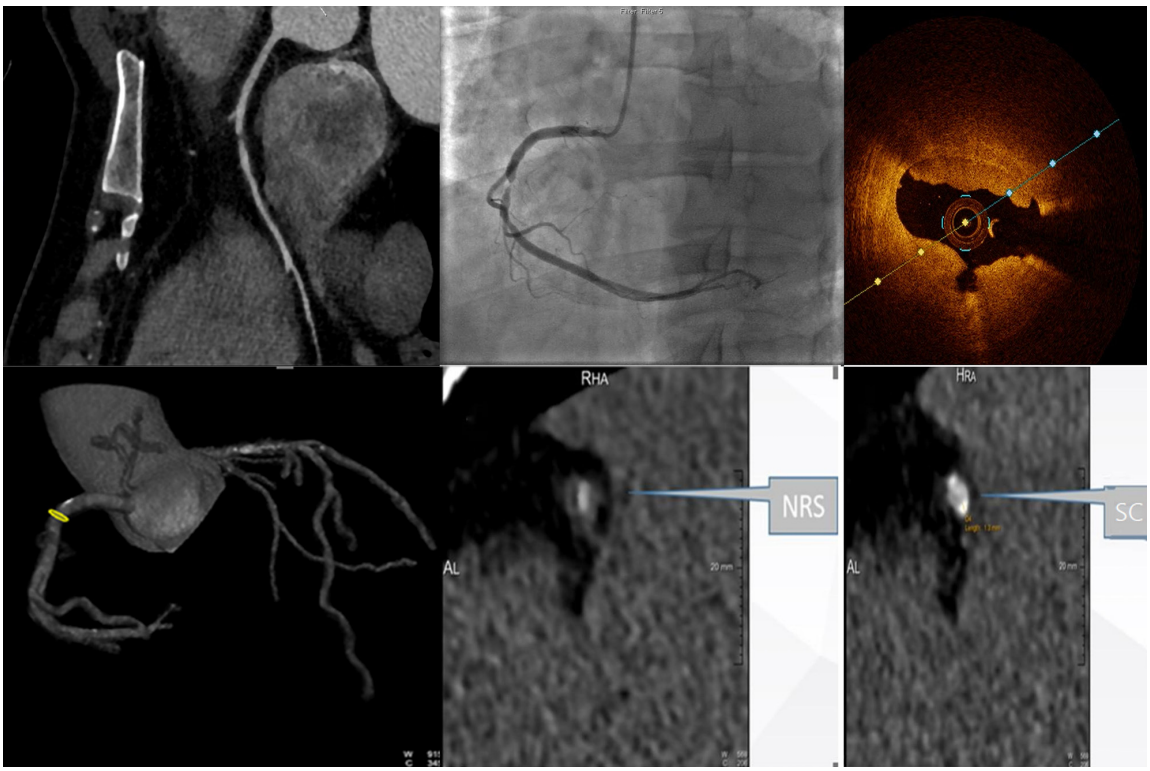

Figure 2 An example of qualitative analysis of plaques. The figure shows the NRS and SC in the sag, cross sectional CCTA images, and OCT images at the same level of lumen where the plaque is located (right corner). NRS, napkin-ring sign; SC, spotty calcification; CCTA, coronary computed tomography angiography; OCT, optical coherence tomography.

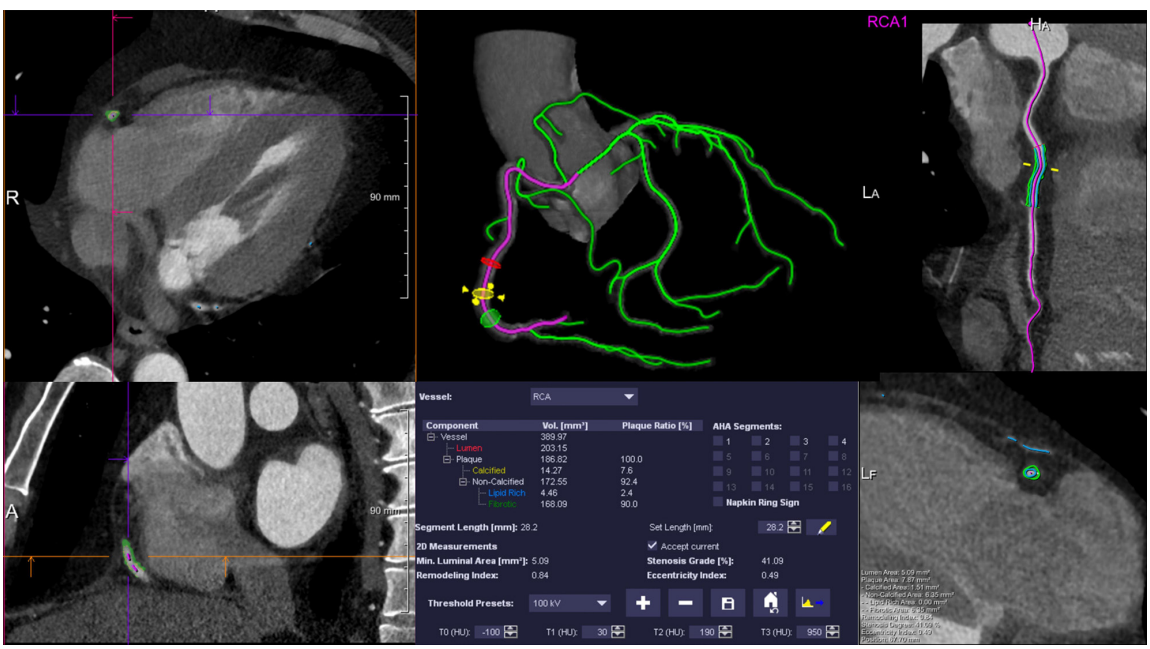

Figure 3 An example of quantitative analysis of plaques. The plaques were quantitatively analyzed by software. RCA, right coronary artery.

Table 3 Univariate logistic regression analysis to assess potential predictors related to vulnerable plaque

Variables	OR	2.5% CI	97.5% CI	P value
NRS	1.725	0.511	5.553	0.363
SC	8.021	2.174	31.520	0.002
LAP	11.571	3.275	45.351	<0.001
PR	3.316	1.049	11.189	0.044
Number of vulnerable plaques signs	1.531	0.579	4.543	0.999
PB	0.193	0.007	5.118	0.321
CPV (m^3)	0.994	0.979	1.004	0.347
CP%	0.992	0.966	1.017	0.558
NCPV (m^3)	1.007	1.000	1.014	0.069
NCP%	1.025	0.997	1.057	0.092
LPV (m^3)	1.043	0.991	1.117	0.126
LP%	1.148	0.990	1.333	0.062
FPV (m^3)	1.007	0.999	1.015	0.071
FP%	1.024	0.995	1.057	0.111
MLA (m^2)	1.031	0.852	1.219	0.729
RI	0.479	0.123	1.327	0.235
EI	1.468	0.148	12.996	0.733
SR (%)	1.013	0.995	1.033	0.179

Number of vulnerable plaques signs is vulnerable plaque number that a plaque had at the same time. OR, odds ratio; CI, confidence interval; NRS, napkin-ring sign; SC, spotty calcification; LAP, low attenuation plaque; PR, positive remodeling; PB, plaque burden; CPV, calcified plaque volume; CP%, calcified plaque ratio; NCPV, non-calcified plaque volume; NCP%, non-calcified plaque ratio; LPV, lipid plaque volume; LP%, lipid plaque ratio; FPV, fibrotic plaque volume; FP%, fibrotic plaque ratio; MLA, minimum lumen area; RI, remodeling index; EI, eccentricity index; SR, stenosis rate.

plaques, whereas LAP can serve as an independent indicator of vulnerable plaques. Ito *et al.* analyzed 122 plaques from 81 patients using OCT results as the gold standard and found that the PR and LAP detected using CCTA were consistent with those diagnosed using OCT (18). Several studies have demonstrated that CCTA has the potential to diagnose vulnerable plaques (19). Interestingly, recent research has shown that the combination of all 4 vulnerable plaque characteristics (NRS, LAP, SC, and PR) in CCTA exhibits the highest accuracy in diagnosing vulnerable plaques (20). Therefore, we herein showed that these features are associated with vulnerable plaques.

A study by Ferencik *et al.* revealed that compared with the volume of plaques in patients with stable angina pectoris (21), the volume of noncalcified plaques in patients with MACEs was higher, which is consistent with the results of this study. NCP% and LP% derived from CCTA were significantly consistent with those of vulnerable plaques derived from OCT. In addition, LP% has been shown to be a potential independent predictor for plaques, and our study demonstrated that FPV could serve as an independent indicator for OCT-defined vulnerable plaques. The higher the LP%, the higher the corresponding LPV. Several previous studies have confirmed that massive calcifications are often clinically stable, and NCPV is an important substrate of MACEs (21,22). According to recent studies, LAP can be used as an independent predictor for vulnerable plaques (23,24). This study, which used OCT as a control, confirmed previous research results. As a result, CCTA has a significant predictive value for adverse cardiac events as well as a good prompting effect on clinical judgment of MACEs and early intervention to prevent the occurrence of

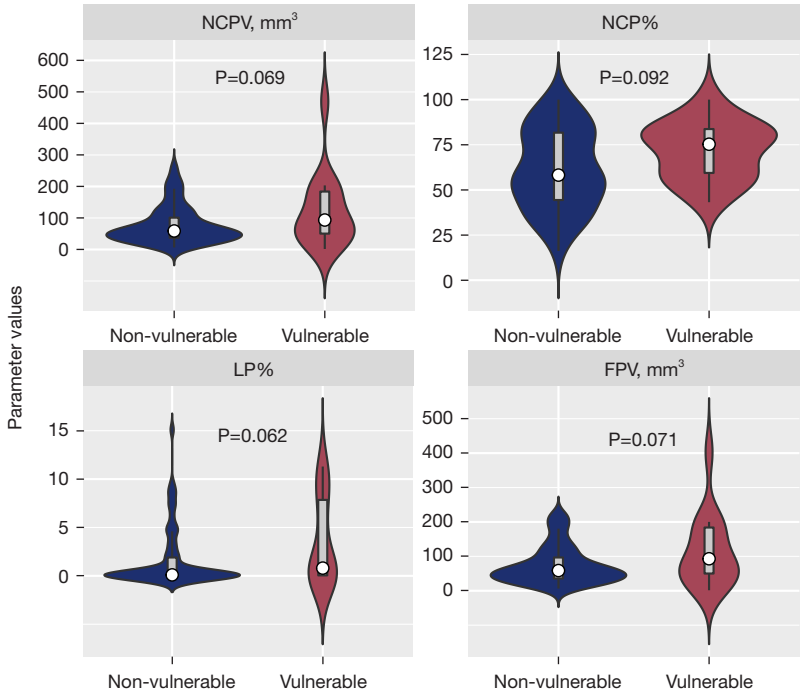

Figure 4 The violin plot in potential predictors of quantitative parameters. Univariate analysis showed that NCPV, NCP%, LP%, and FPV were potential predictors of vulnerable plaques. In the violin plot, the width of the nonvulnerable plaque was larger than that of the vulnerable plaque, which indicated that the distribution of the quantitative parameters was concentrated in the nonvulnerable plaque group and dispersed in the vulnerable plaque group. The quantitative parameters of the NCP% were evenly distributed in the vulnerable and non-vulnerable plaque groups. NCPV, non-calcified plaque volume; NCP%, non-calcified plaque ratio; LP%, lipid plaque ratio; FPV, fibrotic plaque volume.

Table 4 Multivariate logistic regression evaluation of independent predictors and modeling of vulnerable plaques

Models	Predictors	B	S.E.	Wald	P value	OR (95% CI)
Qualitative model	SC	1.509	0.759	3.952	0.047	4.521 (1.022–20.008)
	LAP	2.081	0.702	8.787	0.003	8.012 (2.024–31.718)
Quantitative model	LP%	0.138	0.074	3.482	0.062	1.148 (0.993–1.327)
Mixed model	FPV	0.013	0.005	6.04	0.014	1.013 (1.003–1.024)
	LAP	3.153	0.817	14.91	<0.001	23.416 (4.725–116.055)

S.E., standard error; OR, odds ratio; CI, confidence interval; SC, spotty calcification; LAP, low attenuation plaque; LP%, lipid plaque ratio; FPV, fibrotic plaque volume.

cardiovascular events.

This study indicates that the combination of FPV and LAP has high accuracy in diagnosing vulnerable plaques. Yuan *et al.* revealed that the combination of LAP and epicardial fat features derived from CCTA can be used as an independent predictor for vulnerable plaque lesions diagnosed using intravascular ultrasound (IVUS) (25). Qiao *et al.* revealed that the combination of quantitative plaque parameters and fractional flow reserve can significantly improve the ability to predict plaque progression (26). Previous studies have mostly used quantitative or qualitative parameters alone to verify the performance of CCTA in diagnosing vulnerable plaques; only a few studies have combined the two types of parameters for diagnosing

Table 5 Evaluation of diagnostic efficiency of three models

Models	AUC (95% CI)	P value (DeLong's test)	Accuracy (95% CI)	Sensitivity	Specificity	P value (McNemar test)
Qualitative model	0.80 (0.654–0.941)	0.171	0.544 (0.690–0.881)	1	0.447	0.016
Quantitative model	0.64 (0.528–0.866)	0.022	0.825 (0.519–0.745)	0.5	0.894	<0.001
Mixed model	0.87 (0.808–0.979)	–	0.842 (0.772–0.935)	0.9	0.83	–

Qualitative parameters (SC and LAP) were included in qualitative model; quantitative parameters (LP%) were included for multivariate analysis; LAP and FPV were included in mixed model. AUC, area under the curve; CI, confidence interval; SC, spotty calcification; LAP, low attenuation plaque; LP%, lipid plaque ratio; FPV, fibrotic plaque volume.

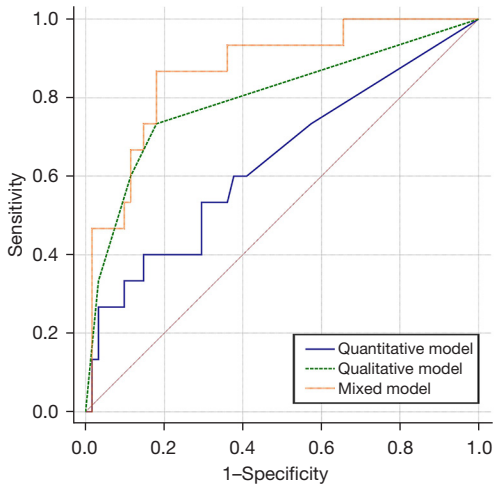

Figure 5 ROC test curve characteristics of quantitative, qualitative, and mixed models. Compared with qualitative and quantitative models, the mixed model, which combined all significant CCTA-derived plaque characteristics, showed the highest AUC and accuracy (mixed model AUC =0.87, qualitative model AUC =0.80, quantitative model AUC =0.64). ROC, receiver operating characteristic; CCTA, coronary computed tomography angiography; AUC, area under the curve.

vulnerable plaques (27,28). In the present study, quantitative and qualitative parameters were combined to diagnose vulnerable plaques (29,30), and OCT was used as a control to improve the accuracy of CCTA in diagnosing vulnerable plaques, confirming the accuracy of CCTA in assessing plaque components.

Several clinical studies have demonstrated the clinical significance of CCTA-derived qualitative and quantitative plaque features (31-33). The accuracy of a semiautomated plaque measurement software for vulnerable plaques from noninvasive CCTA was confirmed in this study. Compared with the use of qualitative or quantitative parameters alone to diagnose vulnerable plaques, a mixed model based on all qualitative and quantitative meaningful parameters showed better diagnostic performance.

The present study has several limitations. Firstly, due to the intricate and costly nature of OCT as a technology with limited clinical applicability, the sample size in this study was relatively small. Additionally, this study solely assessed the diagnostic efficacy of qualitative and quantitative parameters without incorporating variables such as pericoronary adipose tissue content and serological markers. Finally, we excluded heavily calcified lesions, which make accurate plaque assessment with OCT impossible and thus cannot be reasonably included in a head-to-head comparison with CT. Therefore, future studies with a larger sample size and the use of the combination of IVUS and OCT are warranted.

CCTA combined with quantitative and qualitative parameters is more valuable in diagnosing OCT-defined vulnerable plaques. The plaque component analysis results derived from CCTA can be used in patient risk stratification and as routine follow-up and admission examination items for patients with CVD to monitor changes in plaque composition and prevent the occurrence of MACEs.

Acknowledgments

The authors thank Linfeng Li from Siemens Healthineers CT Collaboration for all the help.

Footnote

Reporting Checklist: The authors have completed the STROBE reporting checklist. Available at https://qims.amegroups.com/article/view/10.21037/qims-24-838/rc

Funding: This study was supported by the Scientific Research Fund of Joint Construction Project of Henan Province and Ministry of Medical Science and Technology (No.

SB201901097) and the Henan Provincial Key Laboratory of Cardiology Medical Imaging (No. 2021-44-16).

Conflicts of Interest: All authors have completed the ICMJE uniform disclosure form (available at https://qims.amegroups.com/article/view/10.21037/qims-24-838/coif). Z.X. is an employee of Siemens Healthineers CT Collaboration. The other authors have no conflicts of interest to declare.

Ethical Statement: The authors are accountable for all aspects of the work in ensuring that questions related to the accuracy or integrity of any part of the work are appropriately investigated and resolved. The study was conducted in accordance with the Declaration of Helsinki (as revised in 2013). The study was approved by the Ethics Board of Fuwai Central China Cardiovascular Hospital (2019 Ethical Review No. 9) and the requirement individual consent for this retrospective analysis was waived.

References

1. Benjamin EJ, Blaha MJ, Chiuve SE, Cushman M, Das SR, Deo R, et al. Heart Disease and Stroke Statistics-2017 Update: A Report From the American Heart Association. Circulation 2017;135:e146-603.
2. Fabris E, Berta B, Roleder T, Hermanides RS, IJsselmuiden AJJ, Kauer F, et al. Thin-Cap Fibroatheroma Rather Than Any Lipid Plaques Increases the Risk of Cardiovascular Events in Diabetic Patients: Insights From the COMBINE OCT-FFR Trial. Circ Cardiovasc Interv 2022;15:e011728.
3. Tufaro V, Serruys PW, Räber L, Bennett MR, Torii R, Gu SZ, Onuma Y, Mathur A, Baumbach A, Bourantas CV. Intravascular imaging assessment of pharmacotherapies targeting atherosclerosis: advantages and limitations in predicting their prognostic implications. Cardiovasc Res 2023;119:121-35.
4. Gong P, Almasian M, van Soest G, de Bruin D, van Leeuwen T, Sampson D, Faber D. Parametric imaging of attenuation by optical coherence tomography: review of models, methods, and clinical translation. J Biomed Opt 2020;25:1-34.
5. Kitahara S, Kataoka Y, Miura H, Nishii T, Nishimura K, Murai K, et al. The feasibility and limitation of coronary computed tomographic angiography imaging to identify coronary lipid-rich atheroma in vivo: Findings from near-infrared spectroscopy analysis. Atherosclerosis 2021;322:1-7.
6. Raffel OC, Merchant FM, Tearney GJ, Chia S, Gauthier DD, Pomerantsev E, Mizuno K, Bouma BE, Jang IK. In vivo association between positive coronary artery remodelling and coronary plaque characteristics assessed by intravascular optical coherence tomography. Eur Heart J 2008;29:1721-8.
7. Wang ZQ, Zhang HX, Wu W, Yuan YS, Dou YN, Yin D, Li XS, Jia CF. Combined coronary CT angiography with plain scan for diagnosis of ruptured plaque: comparison with optical coherence tomography. Int J Cardiovasc Imaging 2021;37:3073-80.
8. Chen Q, Pan T, Yin X, Xu H, Gao X, Tao X, Zhou L, Xie G, Kong X, Huang X, Gao N, Zhang JJ, Zhang LJ. CT texture analysis of vulnerable plaques on optical coherence tomography. Eur J Radiol 2021;136:109551.
9. Soeda T, Uemura S, Morikawa Y, Ishigami K, Okayama S, Hee SJ, Nishida T, Onoue K, Somekawa S, Takeda Y, Kawata H, Horii M, Saito Y. Diagnostic accuracy of dual-source computed tomography in the characterization of coronary atherosclerotic plaques: comparison with intravascular optical coherence tomography. Int J Cardiol 2011;148:313-8.
10. Prati F, Regar E, Mintz GS, Arbustini E, Di Mario C, Jang IK, Akasaka T, Costa M, Guagliumi G, Grube E, Ozaki Y, Pinto F, Serruys PW; . Expert review document on methodology, terminology, and clinical applications of optical coherence tomography: physical principles, methodology of image acquisition, and clinical application for assessment of coronary arteries and atherosclerosis. Eur Heart J 2010;31:401-15.
11. Prati F, Guagliumi G, Mintz GS, Costa M, Regar E, Akasaka T, et al. Expert review document part 2: methodology, terminology and clinical applications of optical coherence tomography for the assessment of interventional procedures. Eur Heart J 2012;33:2513-20.
12. Yuan M, Wu H, Li R, Yu L, Zhang J. Epicardial adipose tissue characteristics and CT high-risk plaque features:

correlation with coronary thin-cap fibroatheroma determined by intravascular ultrasound. Int J Cardiovasc Imaging 2020;36:2281-9.
13. Puchner SB, Liu T, Mayrhofer T, Truong QA, Lee H, Fleg JL, Nagurney JT, Udelson JE, Hoffmann U, Ferencik M. High-risk plaque detected on coronary CT angiography predicts acute coronary syndromes independent of significant stenosis in acute chest pain: results from the ROMICAT-II trial. J Am Coll Cardiol 2014;64:684-92.
14. Basha MAA, Aly SA, Ismail AAA, Bahaaeldin HA, Shehata SM. The validity and applicability of CAD-RADS in the management of patients with coronary artery disease. Insights Imaging 2019;10:117.
15. Voros S, Rinehart S, Qian Z, Joshi P, Vazquez G, Fischer C, Belur P, Hulten E, Villines TC. Coronary atherosclerosis imaging by coronary CT angiography: current status, correlation with intravascular interrogation and meta-analysis. JACC Cardiovasc Imaging 2011;4:537-48.
16. Nakazato R, Otake H, Konishi A, Iwasaki M, Koo BK, Fukuya H, Shinke T, Hirata K, Leipsic J, Berman DS, Min JK. Atherosclerotic plaque characterization by CT angiography for identification of high-risk coronary artery lesions: a comparison to optical coherence tomography. Eur Heart J Cardiovasc Imaging 2015;16:373-9.
17. Marano R, Rovere G, Savino G, Flammia FC, Carafa MRP, Steri L, Merlino B, Natale L. CCTA in the diagnosis of coronary artery disease. Radiol Med 2020;125:1102-13.
18. Ito T, Terashima M, Kaneda H, Nasu K, Matsuo H, Ehara M, Kinoshita Y, Kimura M, Tanaka N, Habara M, Katoh O, Suzuki T. Comparison of in vivo assessment of vulnerable plaque by 64-slice multislice computed tomography versus optical coherence tomography. Am J Cardiol 2011;107:1270-7.
19. Ybarra LF, Szarf G, Ishikawa W, Chamié D, Caixeta A, Puri R, Perin MA. Diagnostic Accuracy of 320-Row Computed Tomography for Characterizing Coronary Atherosclerotic Plaques: Comparison with Intravascular Optical Coherence Tomography. Cardiovasc Revasc Med 2020;21:640-6.
20. Kesarwani M, Nakanishi R, Choi TY, Shavelle DM, Budoff MJ. Evaluation of Plaque Morphology by 64-Slice Coronary Computed Tomographic Angiography Compared to Intravascular Ultrasound in Nonocclusive Segments of Coronary Arteries. Acad Radiol 2017;24:968-74.
21. Ferencik M, Pencina KM, Liu T, Ghemigian K, Baltrusaitis K, Massaro JM, D'Agostino RB Sr, O'Donnell CJ, Hoffmann U. Coronary Artery Calcium Distribution Is an Independent Predictor of Incident Major Coronary Heart Disease Events: Results From the Framingham Heart Study. Circ Cardiovasc Imaging 2017;10:e006592.
22. Pu J, Mintz GS, Biro S, Lee JB, Sum ST, Madden SP, Burke AP, Zhang P, He B, Goldstein JA, Stone GW, Muller JE, Virmani R, Maehara A. Insights into echo-attenuated plaques, echolucent plaques, and plaques with spotty calcification: novel findings from comparisons among intravascular ultrasound, near-infrared spectroscopy, and pathological histology in 2,294 human coronary artery segments. J Am Coll Cardiol 2014;63:2220-33.
23. Matsumoto H, Watanabe S, Kyo E, Tsuji T, Ando Y, Otaki Y, Cadet S, Gransar H, Berman DS, Slomka P, Tamarappoo BK, Dey D. Standardized volumetric plaque quantification and characterization from coronary CT angiography: a head-to-head comparison with invasive intravascular ultrasound. Eur Radiol 2019;29:6129-39.
24. Williams MC, Kwiecinski J, Doris M, McElhinney P, D'Souza MS, Cadet S, et al. Low-Attenuation Noncalcified Plaque on Coronary Computed Tomography Angiography Predicts Myocardial Infarction: Results From the Multicenter SCOT-HEART Trial (Scottish Computed Tomography of the HEART). Circulation 2020;141:1452-62.
25. Yuan M, Wu H, Li R, Yu M, Dai X, Zhang J. The value of quantified plaque analysis by dual-source coronary CT angiography to detect vulnerable plaques: a comparison study with intravascular ultrasound. Quant Imaging Med Surg 2020;10:668-77.
26. Qiao HY, Tang CX, Schoepf UJ, Tesche C, Bayer RR 2nd, Giovagnoli DA, Todd Hudson H Jr, Zhou CS, Yan J, Lu MJ, Zhou F, Lu GM, Jiang JW, Zhang LJ. Impact of machine learning-based coronary computed tomography angiography fractional flow reserve on treatment decisions and clinical outcomes in patients with suspected coronary artery disease. Eur Radiol 2020;30:5841-51.
27. Stolzmann P, Schlett CL, Maurovich-Horvat P, Maehara A, Ma S, Scheffel H, Engel LC, Károlyi M, Mintz GS, Hoffmann U. Variability and accuracy of coronary CT angiography including use of iterative reconstruction algorithms for plaque burden assessment as compared with intravascular ultrasound-an ex vivo study. Eur Radiol 2012;22:2067-75.
28. van Assen M, Varga-Szemes A, Schoepf UJ, Duguay TM, Hudson HT, Egorova S, Johnson K, St Pierre S, Zaki B, Oudkerk M, Vliegenthart R, Buckler AJ. Automated plaque analysis for the prognostication of major adverse cardiac events. Eur J Radiol 2019;116:76-83.
29. Boi A, Jamthikar AD, Saba L, Gupta D, Sharma A, Loi

B, Laird JR, Khanna NN, Suri JS. A Survey on Coronary Atherosclerotic Plaque Tissue Characterization in Intravascular Optical Coherence Tomography. Curr Atheroscler Rep 2018;20:33.
30. Kolossváry M, Park J, Bang JI, Zhang J, Lee JM, Paeng JC, Merkely B, Narula J, Kubo T, Akasaka T, Koo BK, Maurovich-Horvat P. Identification of invasive and radionuclide imaging markers of coronary plaque vulnerability using radiomic analysis of coronary computed tomography angiography. Eur Heart J Cardiovasc Imaging 2019;20:1250-8.
31. Zhang X, Nan N, Tong X, Chen H, Zhang X, Li S, Zhang M, Gao B, Wang X, Song X, Chen D. Validation of biomechanical assessment of coronary plaque vulnerability based on intravascular optical coherence tomography and digital subtraction angiography. Quant Imaging Med Surg 2024;14:1477-92.
32. Maurovich-Horvat P, Ferencik M, Voros S, Merkely B, Hoffmann U. Comprehensive plaque assessment by coronary CT angiography. Nat Rev Cardiol 2014;11:390-402.
33. Cao JJ, Shen L, Nguyen J, Rapelje K, Porter C, Shlofmitz E, Jeremias A, Cohen DJ, Ali ZA, Shlofmitz R. Accuracy and limitation of plaque detection by coronary CTA: a section-to-section comparison with optical coherence tomography. Sci Rep 2023;13:11845.

Cite this article as: Liu X, Xie R, Pan Y, Xu Z, Ge Y, Xu J. Assessment of coronary computed tomography angiography-derived plaque features in the diagnosis of optical coherence tomography-defined vulnerable plaques. Quant Imaging Med Surg 2025;15(3):2029-2041. doi: 10.21037/qims-24-838

